Available online at www.sciencedirect.com
ScienceDirect
Journal of Power Sources 179 (2008) 367–370
JOURNAL OF POWER SOURCES
www.elsevier.com/locate/jpowsour

Short communication

A new SiO/C anode composition for lithium-ion battery

Chil-Hoon Doh [a,*], Chul-Wan Park [b], Hye-Min Shin [a], Dong-Hun Kim [a], Young-Dong Chung [a], Seong-In Moon [a], Bong-Soo Jin [a], Hyun-Soo Kim [a], Angathevar Veluchamy [a,c]

[a] *Korea Electrotechnology Research Institute, Changwon 641-120, Republic of Korea*
[b] *SODIFF New Materials, Youngju 750-080, Republic of Korea*
[c] *Central Electrochemical Research Institute, Karaikudi 630006, India*

Received 7 August 2007; received in revised form 11 October 2007; accepted 3 December 2007
Available online 31 December 2007

Abstract

A new anode composition comprising SiO and graphite(C) is prepared through a high-energy ball milling process. During the first cycle, the anode delivers high discharge and charge capacity values of 1556 and 693 mAh g^{-1}, respectively. The electrode shows a reversible charge capacity value of 688 mAh g^{-1} at the 30th cycle with 99% Coulombic efficiency. X-ray diffraction analysis reveals that ball milling does not produce any new compound, but only causes a reduction in particle size. The irreversible and reversible capacities appear to be interdependent.
© 2008 Published by Elsevier B.V.

Keywords: High energy ball milling; SiO/graphite composite; Anode; Li-ion battery

1. Introduction

As miniature electronics and next-generation electric vehicle applications necessitate the development of batteries with high specific energies, the search for high specific capacity electrode materials becomes most important. In order to achieve this, the ability of lithium to form alloys such as $Li_{22}Si_5$ and $Li_{22}Sn_5$, with theoretical capacities of 4190 and 990 mAh g^{-1}, respectively, has been considered with a view to replace the graphite anode which has a specific capacity of 372 mAh g^{-1}. The practical application of both tin and silicon has been hampered as they undergo severe crystallographic changes during alloying and de-alloying processes that cause disintegration of the active materials and loss of electrical contact within the electrode. These effects lead to premature cell failure. The volume variation and crumbling of electrodes were considerably reduced by the development of novel electrode compositions that were capable of absorbing the volume changes. Silicon-based anode materials showed considerable improvement in their electrochemical characteristics when the materials were modified as intermetallic alloys, compounds, nanosized materials or composite materials [1,2].

Among the silicon-based anode materials synthesized and explored [3–11], SiO anodes have shown promising results. H.Y. Lee and S.M. Lee [12] synthesized a nano-Si dispersed oxide anode through mechanochemical milling of SiO, Al and Li_2O_2 and demonstrated a reversible capacity of greater than 550 mAh g^{-1} even at 40th cycle. This demonstrated that the low capacity fade is due to reduced particle size. Morita and Takami [13] prepared a nanosilicon cluster comprised of Si, SiO_x and C through disproportionation of silicon monoxide and polymerization of furfuryl alcohol, and reported a reversible capacity of the order of 700 mAh g^{-1} with a long cycle-life. Later, Yang et al. [14] synthesized a composite of nanosized silicon, Li_4SiO_4 and other lithium-rich components by mechanical reduction of SiO with lithium. The initial and the 50th cycle capacity was 770 and 762 mAh g^{-1}, respectively. Recently, a core Si/SiO nanocomposite anode prepared by a sol–gel method delivered nearly 540 mAh g^{-1} at the 20th cycle [15] and also a carbon-coated SiO anode using polyvinyl alcohol gave a reversible capacity of 710 mAh g^{-1} at the 100th cycle [16].

The preparation procedures reported so far for the synthesis of SiO-based anode involve one or more additional steps that make the process complicated for industrial applications. In this

* Corresponding author. Tel.: +82 55 280 1662; fax: +82 55 280 1590.
E-mail address: chdoh@keri.re.kr (C.-H. Doh).

0378-7753/$ – see front matter © 2008 Published by Elsevier B.V.
doi:10.1016/j.jpowsour.2007.12.074

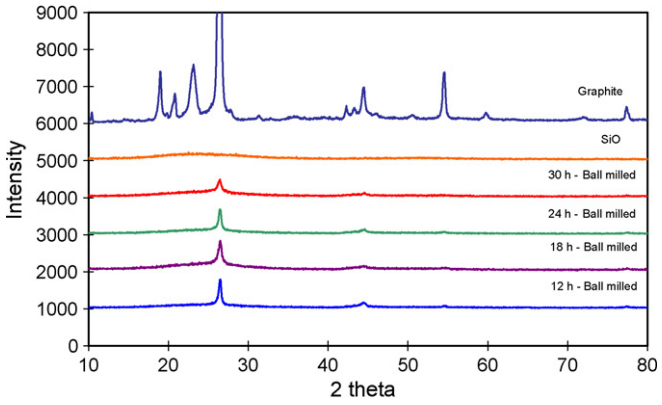

Fig. 1. XRD patterns of SiO, graphite (C), and samples (SiO and graphite) ball-milled for different durations.

study, we report a simple, one-step method for the preparation of a SiO-based composite anode with high specific capacity and also present the physical and electrochemical characterization of the anode materials.

2. Experimental details

Equal proportions of SiO (Aldrich, −325 mesh) and graphite (Sodiff New Materials Co. Ltd., Korea, −400 mesh) powders were placed, together with stainless steel (SS) balls, in a 200 ml stainless steel (SS) vial. The weight ratio of the SS ball to the material was maintained at 10:1 and the vial was filled with argon gas. The contents in the vial were milled for 12, 18, 24 and 30 h by means of high-energy ball milling (HEBM) at 350 rpm and four different samples were collected. A viscous mass was prepared by mixing the milled material with 15 wt.% polyvinylidene difluoride (PVDF) dissolved in 1-methyl-2-pyrrolidinone using an agitator. The viscous mass was coated on a copper foil and dried in a hot air oven at 110 °C for 1 h and then pressed using a stainless steel roller to reduce the thickness to ∼75%. Finally, the film was annealed at 110 °C for 12 h in vacuum.

The active material coated copper foil was cut in the form of a circular disc of diameter 1.4 cm and coupled with a lithium foil counter electrode separated by polypropylene separator of Celgard membrane 2700. The electrolyte (received from Techno Semichem. Ltd., Korea) was 1 M $LiPF_6$ with 2 wt.% vinylene carbonate (VC) dissolved in ethylene carbonate (EC) and ethyl methyl carbonate (EMC) mixed in 1:1 (v/v) ratio. The coin cells were assembled in a dry room maintained at ∼21 °C with a dew point temperature ∼−65 °C. The anode was cycled between 0 and 1.5 V versus Li^+/Li at a constant current of 0.253 mA cm^{-2} using a charge–discharge analyzer, Toyo System Ltd., Japan.

The composite powders were examined with a Philips 1830 X-ray diffractometer with nickel-filtered Cu Kα radiation at a scan rate of 0.04 ° per second over a 2Θ range of 10°–80°. The surface morphology of the active material coated on copper foil was scanned with a Hitachi S-4800 scanning electron microscope.

3. Results and discussion

The XRD patterns obtained for SiO, graphite(C) and milled SiO/C composites are presented in Fig. 1. The pattern shows that the graphite considered for ball milling is crystalline whereas

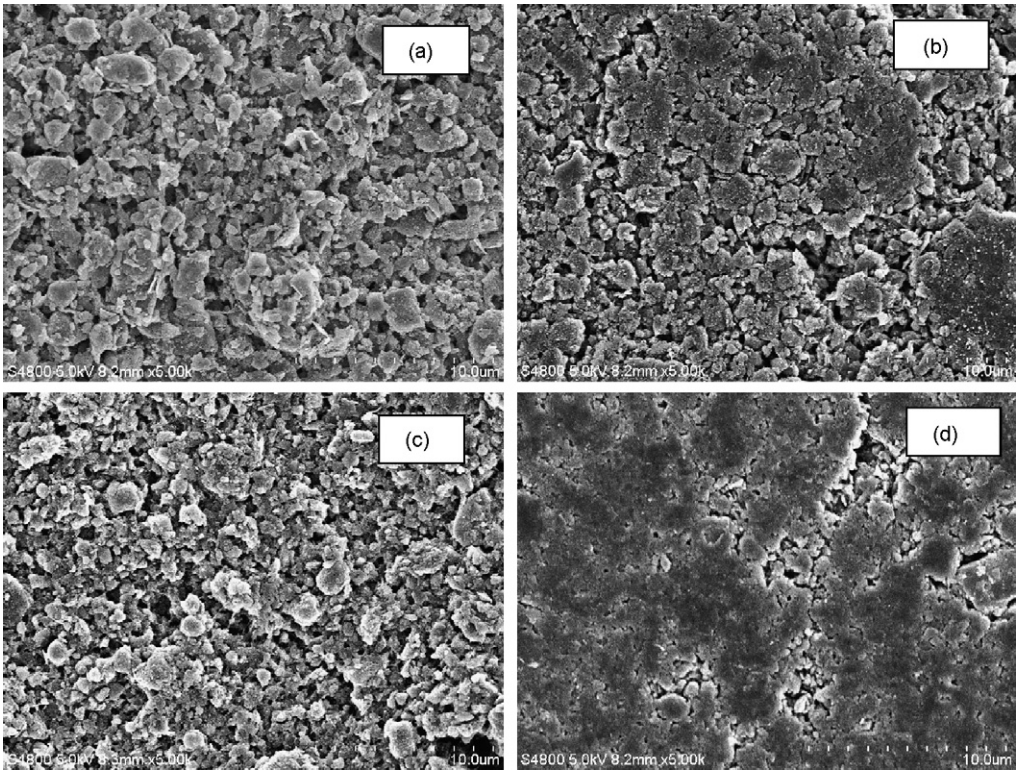

Fig. 2. SEM micrographs of samples (SiO and graphite) ball-milled for different durations: (a) 12 h; (b) 18 h; (c) 24 h; (d) 30 h.

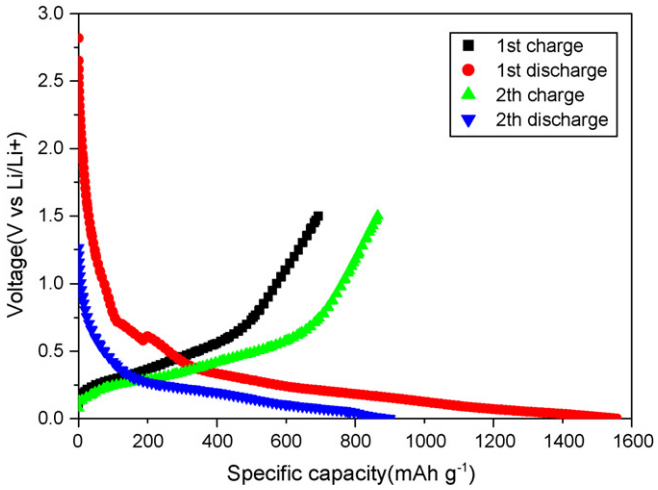

Fig. 3. Voltage as function of specific capacity for an electrode made from a sample ball-milled for 24 h.

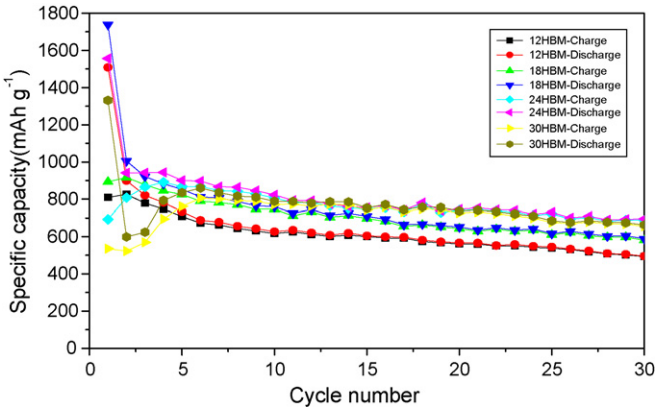

Fig. 4. Specific capacity as function of cycle number at different ball mill durations.

SiO is amorphous. The patterns for milled SiO/C samples reveal that the peak corresponding to graphite decreases with increase in ball mill duration and also no new peaks observed. This suggests that ball milling causes only particle size reduction of the graphite and does not produce any new compound.

Scanning electron micrographs of samples ball-milled for different durations are given in Fig. 2. A gradual decrease in the crystallinity of the particulates of the samples with ball mill duration is observed in accordance with the XRD patterns. The particles in the sample milled for 12 h exist as discrete crystalline particles whereas the 30 h-milled sample lacks definite particle shape and shows continuity in the particle distribution. In some domains, the particle distribution in the 24 h ball-milled sample remains between 5 and 20 μm whereas in other regions continuity is maintained.

A typical discharge–charge profile of the SiO/C composite electrode is given in Fig. 3. The difference between the initial discharge (1556 mAh g^{-1}) and charge (693 mAh g^{-1}) capacities gives the irreversible capacity as 55%. In the second cycle, the irreversible capacity is reduced to 14%. It is well known that during the first lithiation process, lithium reacts with SiO and this leads to the formation of nanosilicon and Li_2O. The nanosilicon then reacts with Li and forms Li–Si alloy [12]. Contrary to this explanation Miyachi et al. [17] showed through O 1s spectra analysis that during the first lithiation process a direct absorption of Li by SiO takes place and gives rise to the formation of Li_4SiO_4 and Li_2O. Hence, the lithiated product responsible for the reversible process may either be Li–Si alloy or Li_4SiO_4. The total irreversible capacity originates from three sources, namely, the reaction of Li with SiO, oxygen present in graphite and other impurities, and decomposition of the electrolyte during initial charging to form a solid electrolyte interface (SEI) film [18–20].

The specific capacity as a function of cycle number for samples milled for different times is given in Fig. 4. The superior cycleability of the present composition may be explained by considering the formation of Li_4SiO_4 rather than Li–Si alloy as the volume expansion of the former is lower than that of the latter during cycling [17]. The discharge and charge capacity values of the initial and 30th cycles obtained from Fig. 4 are listed in Table 1. The reversible and irreversible capacity values appear to be interdependent as their values show simultaneous increase until the 24 h ball-milled sample. This interdependency also explains the beneficial role played by a higher percentage of Li_2O which buffers the volume expansion during the alloying and de-alloying processes. Among the composites, the 24 h ball-milled sample exhibits higher reversible capacity possibly due to optimum particle size distribution for better lithium ion diffusion compared with the others. The loss of capacity shown by the sample with cycling may be attributed to trapping of Li^+ ions in the electrode particles and decomposition of the organic solvent to form an SEI film. The other factors responsible for capacity degradation with cycle-life are particle fracture and loss of electrical contact between the electro-active species and current-collector.

The discharge–charge capacity and the Coulombic efficiency curve for the 24 h ball-milled sample are depicted in Fig. 5. The curve shows that the electrode exhibits high charge–discharge capacity with a Coulombic efficiency of ∼99% at the 30th

Table 1
Capacity values at 1st and 30th cycle at different ball mill duration

Ball mill duration (h)	1st cycle			30th cycle	
	Discharge capacity (mAh g^{-1})	Charge capacity (mAh g^{-1})	Irreversible capacity (%)	Discharge capacity (mAh g^{-1})	Charge capacity (mAh g^{-1})
12	1508	809	46	495	493
18	1738	892	48	589	580
24	1556	693	55	696	688
30	1330	535	59	663	656

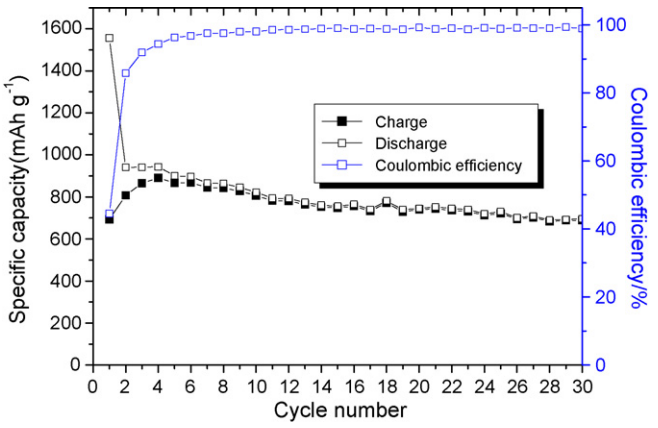

Fig. 5. Charge–discharge capacity and Coulombic efficiency with cycle number for electrode made from a 24 h ball-milled sample.

cycle. These results are comparable with those of other workers [13,14].

4. Conclusions

The high reversible capacity of ~690 mAh g^{-1} with a Coulombic efficiency of ~99% hitherto unreported for the new SiO/C (50:50) composite is unique in the sense that it does not involve any additional process or incorporation of a third element. This investigation also shows the interdependency of the irreversible and reversible capacity of the SiO-based system. Phase characterization of SiO/C reveals that ball milling does not produce any alloy or compound and that the electrode constituents remain only in elemental states.

Acknowledgements

This work has been carried out at Division of Advanced Batteries supported by the NGE program (Project No. 1001653) of KERI, Korea. One of the authors, A. Veluchamy, wishes to thank the Korean Federation of Science and Technology Societies, Korea for the award of a Brain Pool Fellowship and is also grateful to CECRI/CSIR, India, for granting leave.

References

[1] N. Dimov, S. Kugino, M. Yoshio, Electrochim. Acta 48 (2003) 1579.
[2] R. Yazami, K. Zaghib, M. Deschamps, J. Power Sources 52 (1994) 55.
[3] M.S. Park, S. Rajendran, Y.M. Kang, K.S. Han, Y.S. Han, J.Y. Lee, J. Power Sources 158 (2006) 650.
[4] H.Y. Lee, Y.L. Kim, M.K. Kong, S.M. Lee, J. Power Sources 141 (2005) 159.
[5] M.S. Park, Y.J. Lee, Y.S. Han, J.Y. Lee, Mater. Lett. 60 (2006) 3079.
[6] P. Zuo, G. Yin, J. Alloys Compds. 414 (2006) 265.
[7] X.D. Wu, Z.X. Wang, L.Q. Chen, X.J. Huang, Electrochem. Commun. 5 (2003) 935.
[8] H. Dong, X.P. Ai, H.X. Yang, Electrochem. Commun. 5 (2003) 952.
[9] P. Patel, I.S. Kim, P.N. Kumta, Mater. Sci. Eng. B 116 (2005) 347.
[10] J.N. Jayaprakash, N. Kalaiselvi, C.H. Doh, Intermetallics 15 (2007) 442.
[11] N. Kalaiselvi, C.H. Doh, C.W. Park, S.I. Moon, M.S. Yun, Electrochem. Commun. 9 (2004) 1110.
[12] H.Y. Lee, S.M. Lee, Electrochem. Commun. 6 (2004) 465.
[13] T. Morita, N. Takami, J. Electrochem. Soc. 153 (2) (2006) A425.
[14] X. Yang, Z. Wen, X. Xu, B. Lin, S. Huang, J. Power Sources 164 (2007) 880.
[15] T. Zhang, J. Gao, H.P. Zhang, L.C. Yang, Y.P. Wu, H.Q. Wu, Electrochem. Commun. 9 (2007) 886.
[16] J.H. Kim, H.J. Sohn, H. Kim, G. Jeong, W. Choi, J. Power Sources 170 (2007) 456.
[17] M. Miyachi, H. Yamamoto, H. Kawai, T. Ohta, M. Shirakata, J. Electrochem. Soc. 153 (10) (2006) A2089–A2091.
[18] D. Aurbach, in: W.A. Schalkwijk, B. Scrosati (Eds.), Advances in Lithium Ion Batteries, Kluwer Academic, New York, 2002, pp. 79–101.
[19] P.B. Balbuena, Y. Wang (Eds.), Lithium Ion Batteries—Solid Electrolyte Interphase, Imperial College Press, London, 2004.
[20] M.K. Datta, P.N. Kumta, J. Power Sources 165 (2007) 368.